

# Analytical approach to directed sandpile models on the Apollonian network

André P. Vieira<sup>1</sup>, José S. Andrade Jr.<sup>2,3</sup>, Hans J. Herrmann<sup>2,3</sup>, and Roberto F. S. Andrade<sup>4</sup>

<sup>1</sup>*Departamento de Engenharia Metalúrgica e de Materiais,*

*Universidade Federal do Ceará, Campus do Pici, 60455-760, Fortaleza, Brazil*

<sup>2</sup>*Departamento de Física, Universidade Federal do Ceará, Campus do Pici, 60455-760, Fortaleza, Brazil*

<sup>3</sup>*Computational Physics, IfB, ETH-Hönggerberg, Schafmattstr. 6, 8093, Zürich, Switzerland*

<sup>4</sup>*Instituto de Física, Universidade Federal da Bahia, 40210-340, Salvador, Brazil*

(Dated: May 26, 2019)

We investigate a set of directed sandpile models on the Apollonian network, which are inspired on the work by Dhar and Ramaswamy (PRL **63**, 1659 (1989)) for Euclidian lattices. They are characterized by a single parameter  $q$ , that restricts the number of neighbors receiving grains from a toppling node. Due to the geometry of the network, two and three point correlation functions are amenable to exact treatment, leading to analytical results for the avalanche distributions in the limit of an infinite system, for  $q = 1, 2$ . The exact recurrence expressions for the correlation functions are numerically iterated to obtain results for finite size systems, when larger values of  $q$  are considered. Finally, a detailed description of the local flux properties is provided by a multifractal scaling analysis.

## I. INTRODUCTION

The interaction networks of many real systems with large number of basic units are often found to display power-law distribution of node degrees and small-world property [? ?]. Examples stem from most different areas, as electric power distribution, food webs in ecology, information flow in the internet, interaction among financial institutions, and so on [? ?]. In recent years, complex networks have also attracted attention as alternative topological structures to ordered euclidian lattices, on which many physical models can be defined. These structures offer a suitable scenario to mimic the effect of geometry in real systems, and have already been used in the investigation of the properties of magnetic [? ? ?] and electron [?] systems.

Understanding the stability of complex networks becomes of relevance for the management of natural and human built systems, as it can provide guidelines to avoid an irreversible collapse and to enhance the robustness of their structure. Another issue that deserves attention is the occurrence of events that may cause permanent or temporary damages on the network, which can be interpreted as avalanches within the proposed self-organized criticality (SOC) scenario [?]. It is well known that a typical signature of SOC systems is the possibility of occurrence of a very large avalanche that can extend itself over the whole network, causing its breakdown. Specific sandpile models defined on complex networks have been recently investigated [?], as well as models where the network is not fixed, but the set of connections evolves slowly with time [?]. In the first case, avalanches refer to the motion of mass units from one node to its neighbors, while in the last approach, avalanches refer to bursts of rewiring connections among the network nodes. It is noteworthy the recent attempts to use SOC concepts with respect to brain activity, both in Euclidian and scale-free networks [? ? ?].

It is well known that direct models, like the one proposed by Dhar and Ramaswamy [?], constitute one of the few classes of SOC models that can be exactly solved on Euclidian lattices. This is essentially related to their Abelian property, according to which the effect of two successive grain additions

on the lattice does not depend on the order. In the context of complex networks, the Apollonian packing problem [?] inspired the introduction of the so-called Apollonian network [? ?]. Besides displaying both scale free and small-world features, the hierarchical geometry of this network enables the derivation of tractable analytical expressions for a variety of equilibrium and dynamical models [?]. This leads either to exact results or to recurrence relations that can be numerically iterated.

In this work, we analyze the avalanches of directed sandpile models on the Apollonian network. We make use of properties of these specific network and model to derive, in a first place, a series of exact results for the distribution of avalanches. Then, these results can be extended, with the help of the numerical iteration of the obtained recurrence relations, to illustrate more general situations. More precisely, we are able to investigate the fine details of the local mass flux, deriving the appropriate multifractal spectra that describe the scaling properties of the flux.

This work is organized as follows: In Section II we introduce our model, discussing the role played by the number of levels  $q$ , in the Apollonian hierarchy, that limit which nodes can receive mass from a toppling neighbor. We also derive the basic expressions for the two and three-point correlation functions that allow for the derivation of the local and total fluxes. Results for the total flux, obtained by numerical iteration, are discussed in Section III, for  $1 \leq q \leq 6$ . They are then compared with analytical expressions derived for the  $q = 1$  and  $q = 2$ . In Section IV, a multifractal approach is used to present the scaling properties of the flux for the distinct values of  $q$ . Finally, Section V closes the paper with our concluding remarks.

## II. DIRECTED SANDPILE MODELS ON THE APOLLONIAN NETWORK

The planar Apollonian network [?] is obtained from the classical Apollonian space-filling packing of circles [?], by associating nodes with the centers of the circles, and draw-

ing edges between nodes corresponding to pairs of touching circles. This iterative building process is illustrated in Fig. 1.

The directed sandpile model of Dhar and Ramaswamy [?] associates with each site  $\mathbf{x}$  of a hypercubic lattice a height variable  $z(\mathbf{x})$ , which is increased by 1 when a grain is added to  $\mathbf{x}$ . If  $z(\mathbf{x})$  exceeds a critical value  $z_c$ , the site topples, and the height variables at the  $\ell$  nearest neighbors of  $\mathbf{x}$  along a preferred direction increase by 1, while  $z(\mathbf{x})$  decreases by  $\ell$ . Without loss of generality,  $z_c$  can be chosen to equal  $\ell$ . The existence of a preferred direction is essential to the exact solvability of the model, not only in its original form but also in generalized versions [? ].

In the Apollonian network, the building process offers an obvious choice of a preferred direction. We define the  $n$ th layer of the network as the set of sites added in the  $n$ th iteration of the process, and we postulate that, when a site at a given layer topples, only sites in subsequent layers can receive grains. However, the Apollonian network has the peculiar property that each site in a given layer is connected to at least one site in each subsequent layer. Thus, in the thermodynamic limit, any site has an infinite number of neighbors in subsequent layers, leading to an infinite critical height. In order to obtain a finite value of  $z_c$ , we impose the restriction that only neighbors in the first  $q$  subsequent layers can receive grains when a site topples, the remaining connections being inactive; see Fig. 2. This leads to a  $q$ -dependent value of the critical height  $z_c$ , which is the same for all sites in the network, provided we forbid the addition of grains to the sites in the original triangle (layer  $n = 0$ ). (For  $q$  from 1 to 6, we have  $z_c = 3, 9, 21, 45, 93$ , and 189.) Thus, all allowed sites have an equivalent set of neighbors in their subsequent layers, and we can study the properties of avalanches by choosing any reference site  $\mathbf{x}_0$ . For convenience, we choose  $\mathbf{x}_0$  to be the site located at the geometrical center of the network (layer  $n = 1$ ).

As in the original directed sandpile model, we define a two-point correlation function  $G_0(\mathbf{x}; \mathbf{x}_0)$  which measures the probability that a site  $\mathbf{x}$  topples in the SOC state due to an avalanche originated by adding a grain at  $\mathbf{x}_0$ . Since the probability that a site topples, provided that  $r$  of its backwards neighbors have toppled, is equal to  $r/z_c$ ,  $G_0$  obeys the recursion equation

$$G_0(\mathbf{x}; \mathbf{x}_0) = \frac{1}{z_c} \left[ \sum_{\mathbf{y}}' G_0(\mathbf{y}; \mathbf{x}_0) + \delta_{\mathbf{x}, \mathbf{x}_0} \right], \quad (1)$$

with the primed summation running over all sites from which  $\mathbf{x}$  can receive grains, according to the  $q$ -layer rule. Since

$$G_0(\mathbf{x}_0; \mathbf{x}_0) = \frac{1}{z_c}, \quad (2)$$

the existence of a preferred direction allows us to solve Eq. (1) for all  $G_0(\mathbf{x}; \mathbf{x}_0)$ , at least numerically.

The flux through the  $n$ th layer is given by

$$\phi(n) = \sum_{\mathbf{x} \in n} G_0(\mathbf{x}; \mathbf{x}_0). \quad (3)$$

Contrary to what is observed in hypercubic lattices, here  $\phi(n)$  generally depends on  $n$ , although it becomes asymptotically

constant for  $n \gg 1$ , as we show below by numerical and analytical calculations. If  $m(n)$  is the average number of sites in the  $n$ th layer that topple when at least one of them does, we can write

$$\phi(n) = m(n)p(n), \quad (4)$$

in which  $p(n)$  is the probability that, in the SOC state, an avalanche started at  $\mathbf{x}_0$  reaches layer  $n$ .

If we assume that

$$p(n) \sim n^{-\alpha}, \quad (5)$$

with some exponent  $\alpha$ , the asymptotic constancy of  $\phi(n)$  allows us to conclude that

$$m(n) \sim \frac{1}{p(n)} \sim n^\alpha. \quad (6)$$

Thus, the average mass of an avalanche reaching  $n$  layers scales as

$$M(n) = \sum_{t=1}^n m(t) \sim \int_1^n dt t^\alpha \sim n^{\alpha+1}, \quad (7)$$

and the probability that the total mass of an avalanche exceeds  $M$  can be written as

$$\hat{p}(M) = p(n(M)) \sim M^{-\frac{\alpha}{1+\alpha}}. \quad (8)$$

Finally, we obtain for  $\rho(M)$ , the probability distribution of avalanches with size  $M$ ,

$$\rho(M) = \frac{d\hat{p}(M)}{dM} \sim M^{-\frac{1+2\alpha}{1+\alpha}} \equiv M^{-\tau}. \quad (9)$$

The exponent  $\alpha$  can be calculated from the mean square flux

$$\Phi(n) = [m(n)]^2 p(n) \sim n^\alpha, \quad (10)$$

which is related to the three-point correlation function  $G(\mathbf{x}_1, \mathbf{x}_2; \mathbf{x}_0)$ , defined as the probability that sites  $\mathbf{x}_1$  and  $\mathbf{x}_2$ , both in the same layer, topple due to an avalanche started by adding a grain at site  $\mathbf{x}_0$ . Explicitly, we have

$$\Phi(n) = \sum_{\mathbf{x}_1, \mathbf{x}_2 \in n} G(\mathbf{x}_1, \mathbf{x}_2; \mathbf{x}_0). \quad (11)$$

As in the case of  $G_0(\mathbf{x}; \mathbf{x}_0)$ , we can write for  $G(\mathbf{x}_1, \mathbf{x}_2; \mathbf{x}_0)$  a recursion equation,

$$G(\mathbf{x}_1, \mathbf{x}_2; \mathbf{x}_0) = \frac{1}{z_c^2} \sum_{\mathbf{y}_1, \mathbf{y}_2}' G(\mathbf{y}_1, \mathbf{y}_2; \mathbf{x}_0), \quad (12)$$

with the primed summation running over all sites from which  $\mathbf{x}_1$  or  $\mathbf{x}_2$  can receive grains, according to the  $q$ -layer rule. This last equation can be solved by the *Ansatz* [? ? ]

$$G(\mathbf{x}_1, \mathbf{x}_2; \mathbf{x}_0) = \sum_{\mathbf{y}} f(\mathbf{y}; \mathbf{x}_0) G_0(\mathbf{x}_1; \mathbf{y}) G_0(\mathbf{x}_2; \mathbf{y}), \quad (13)$$

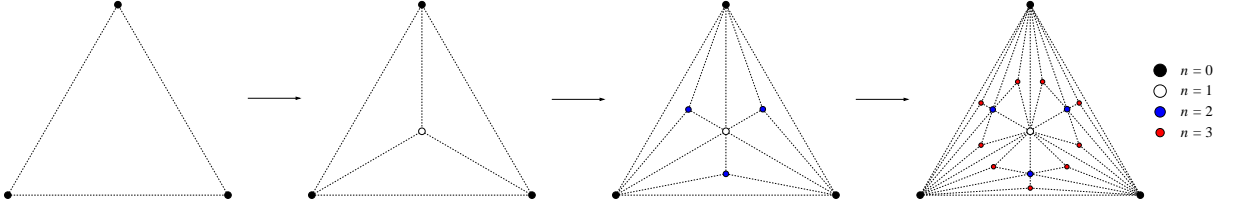


Figure 1: Building process of the Apollonian network.

with the function  $f(\mathbf{y}; \mathbf{x}_0)$  determined by the condition

$$G(\mathbf{x}, \mathbf{x}; \mathbf{x}_0) = G_0(\mathbf{x}; \mathbf{x}_0), \quad (14)$$

which leads to

$$\sum_{\mathbf{y}} f(\mathbf{y}; \mathbf{x}_0) G_0(\mathbf{x}; \mathbf{y}) G_0(\mathbf{x}; \mathbf{y}) = G_0(\mathbf{x}; \mathbf{x}_0). \quad (15)$$

Summing over all sites  $\mathbf{x}$  in the same layer  $n$ , using Eq. (3) and the fact that  $G(\mathbf{x}; \mathbf{y}) = G(\mathbf{x} - \mathbf{y} + \mathbf{x}_0; \mathbf{x}_0)$ , we can rewrite Eq. (15) as

$$\sum_{t=1}^n F(t) K(n-t+1) = \phi(n), \quad (16)$$

in which

$$F(t) = \sum_{\mathbf{y} \in t} f(\mathbf{y}) \quad \text{and} \quad K(t) = \sum_{\mathbf{x} \in t} G_0(\mathbf{x}; \mathbf{x}_0) G_0(\mathbf{x}; \mathbf{x}_0). \quad (17)$$

Starting from  $n = 1$ , Eq. (16) can be solved recursively for  $F(n)$ . By substituting Eq. (13) into Eq. (11), we can express  $\Phi(n)$  in terms of  $F(n)$ ,

$$\Phi(n) = \sum_{t=1}^n F(t) [\phi(n-t+1)]^2. \quad (18)$$

The scaling behavior of  $\Phi(n)$  determines the exponent  $\alpha$ .

The case  $q = 1$  is immediately solved. In this limit, the Apollonian network (with the three original vertices removed) reduces to a Cayley tree with coordination number equal to 4, as shown in Fig. 2. The two-point correlation is easily seen to satisfy

$$G_0(\mathbf{x}; \mathbf{x}_0) = \frac{1}{3^n}, \quad \mathbf{x} \in n, \quad (19)$$

so that the average flux is  $\phi(n) = 1/3, \forall n$ , leading to

$$K(n) = \frac{1}{3^{n+1}}, \quad F(1) = 3, \quad F(n) = 2 \quad (n > 1). \quad (20)$$

Thus, the mean square flux is given by

$$\Phi(n) = \frac{1}{9} + \frac{2}{9}n, \quad (21)$$

corresponding to  $\alpha = 1(\tau = 3/2)$ , characteristic of the mean-field behavior associated with the directed model in Bravais lattices with dimension  $d \geq 4$ . For the purpose of comparison, the corresponding exact values in  $d = 2$  are  $\alpha = 1/2, \tau = 4/3$ .

In the next two sections, we discuss the properties of the model for  $q > 1$ .

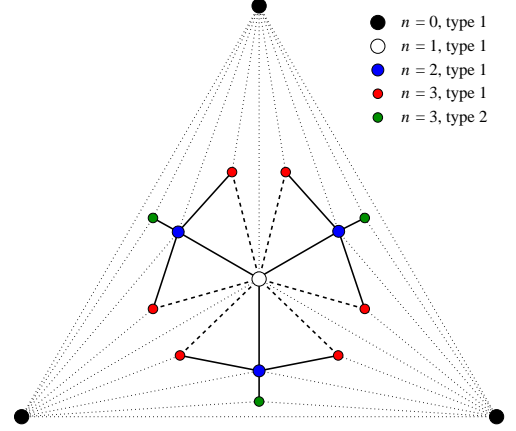


Figure 2: Apollonian network with  $q = 2$ . Dotted lines correspond to inactive connections; thick lines indicate connections between sites in adjacent layers, while dashed lines connect sites separated by 2 layers. Note that there are two types of sites in layer  $n = 3$ . If  $q = 1$ , also dashed lines become inactive.

### III. AVERAGE BEHAVIOR

For  $q \geq 2$ , sites in the same layer are no longer equivalent, since we are preserving the underlying topology of the Apollonian network as defined by the building rule. Instead, those sites are naturally grouped in different classes, defined by the structure of their connection to sites in previous layers. In principle, this makes the model amenable to analytical treatment. As we show in Appendix A, the analysis for  $q = 2$  is already somewhat intricate, but it lends support to a series of conclusions we obtain by numerical calculations. These are performed by building an Apollonian network with up to 16 layers (corresponding to 21 523 363 sites), imposing the  $q$ -layer rule, and solving recursively Eqs. (1) and (16). From this, we can calculate both the mean flux  $\phi(n)$  and the mean square flux  $\Phi(n)$  as functions of the layer index  $n$ . (In Sec. IV we study the local properties of the flux.)

The first conclusion to emerge from our numerical analysis is that the mean flux  $\phi(n)$  becomes asymptotically constant for large  $n$ , as already mentioned in Sec. II. This is evident in Fig. 3(a), where we plot, for several values of  $q$ , the ratio between  $\phi(n)$  and the corresponding (constant) result for  $q = 1$ . Notice the oscillations in  $\phi(n)$  for small values of  $n$ . These are related to the fact that, as the number of neighbors of a site in a given subsequent layer increases with the layer index, so does the fraction of grains received by each layer when the

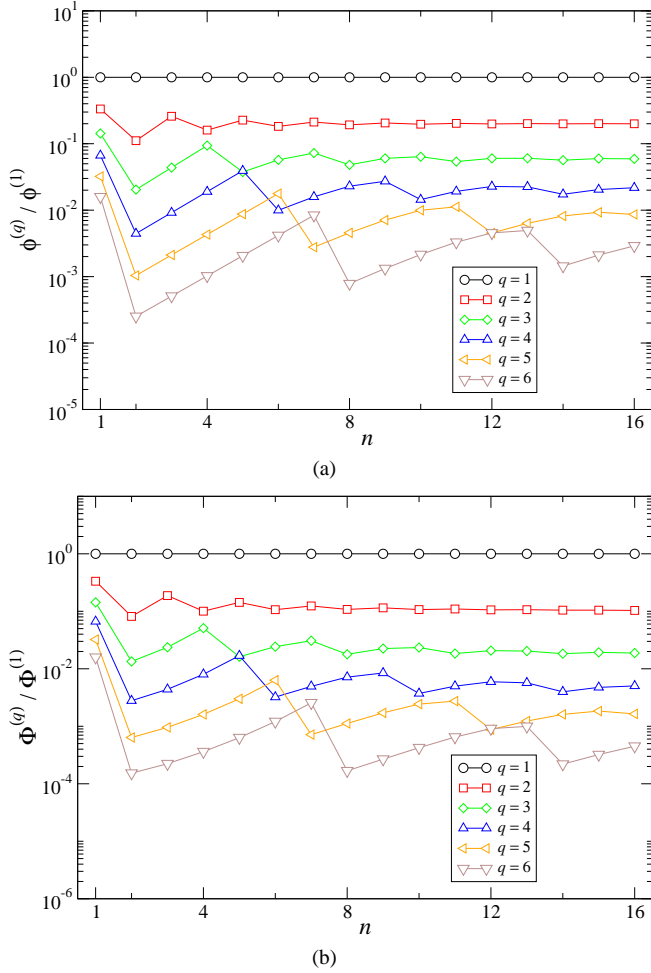


Figure 3: (a) Mean flux as a function of the layer index  $n$ , for different values of  $q$ , divided by the mean flux for  $q = 1$ . (b) Corresponding curves for the mean square flux.

site topples. Since we have a single site through which grains enter the system (in layer  $n = 1$ ), we note that, for  $q > 1$ , the mean flux reaching layer  $n = 2$  drops in comparison with the total flux, then increases from  $n = 2$  to  $n = q + 1$ , dropping again for  $n = q + 2$ . But this second drop is smaller, because sites in that layer receive grains from all  $q$  previous layers. As a result of this process, the oscillations are smoothed out for sufficiently high values of  $n$ .

Corresponding curves for the mean square flux are shown in Fig. 3(b). Again the curves oscillate for small values of the layer index  $n$ , but approach a constant value for large  $n$ , showing that  $\Phi(n)$  always satisfies the scaling form

$$\Phi(n) \sim n. \quad (22)$$

This means that asymptotically the distribution of avalanche sizes follows a power-law with exponent  $\alpha = 1$ , irrespective of  $q$ .

This prevalence of a mean-field behavior could be anticipated on the basis of the tree-like topology of the lattice obtained by imposing the  $q$ -layer rule. A similar situation arises

in other sandpile models on different forms of decorated Cayley trees [? ? ]; since the correlation length is infinite in the SOC state, the mean-field behavior characteristic of the ordinary Cayley tree (or more precisely the Bethe lattice) is recovered.

In the Apollonian network, the  $q$ -layer rule defines a typical length beyond which average properties become indistinguishable from those of the model on a Cayley tree. However, at smaller scales, hints of the behavior corresponding to the genuine Apollonian network do appear, for instance in the oscillations observed in the mean-flux curves. As clearly shown in Fig. 3(a),  $\phi(n)$  depends exponentially on  $n$  between  $n = 2$  and  $n = q + 1$ ,

$$\phi(n) = Ae^{an}, \quad (23)$$

with a  $q$ -dependent prefactor  $A$ , but a nearly constant value of  $a \simeq 0.7$ . The prefactor  $A$  decreases exponentially with  $q$ , since it is related to the inverse threshold height  $1/z_c$ . The exponential (rather than linear) dependence of  $\phi(n)$  is a consequence of the exponential increase in the number of neighbors as a function of the layer separation. In the  $q \rightarrow \infty$  limit, the central site topples only after the addition of an enormous number of grains, most of which are then received by sites in very distant layers. As a consequence, all avalanches have arbitrarily large range.

#### IV. MULTIFRACTAL PROPERTIES OF THE FLUX

Although the average behavior of the flux reproduces that of the mean-field limit, the local-flux distribution reveals interesting properties already for  $q = 2$ . In Fig. 4(a) we plot histograms of the local flux  $\phi$  for  $n = 22$ . Note that, due to a precise identification of the distinct types of sites for the  $q = 2$  model, we were able to consider much larger number of nodes ( $> 10^{10}$ ) than for the results reported in the previous section. The fluxes are re-scaled by the corresponding maximum flux  $\phi_{\max}$  in that layer.

In analogy with studies on the distribution of currents in the incipient infinite cluster of a random-resistor network [? ], it is interesting to evaluate the moments of the flux, in order to better reveal the scaling properties hidden in Fig. 4(a). So we use the definition

$$\overline{M}_k(n) = \sum_{\mathbf{x} \in n} \left( \frac{\phi_{\mathbf{x}}}{\phi_0} \right)^k, \quad (24)$$

in which the summation runs over all sites  $\mathbf{x}$  in the  $n$ th layer of the Apollonian network,

$$\phi_{\mathbf{x}} \equiv G_0(\mathbf{x}; \mathbf{x}_0) \quad (25)$$

and  $\phi_0$  is the initial flux. It turns out that, for all real values of  $k$ , the moments satisfy scaling relations given by

$$\overline{M}_k(n) \sim e^{u_k n}, \quad (26)$$

with well defined coefficients  $u_k$ , so that, in terms of the system size

$$L \sim 3^{n+1}, \quad (27)$$

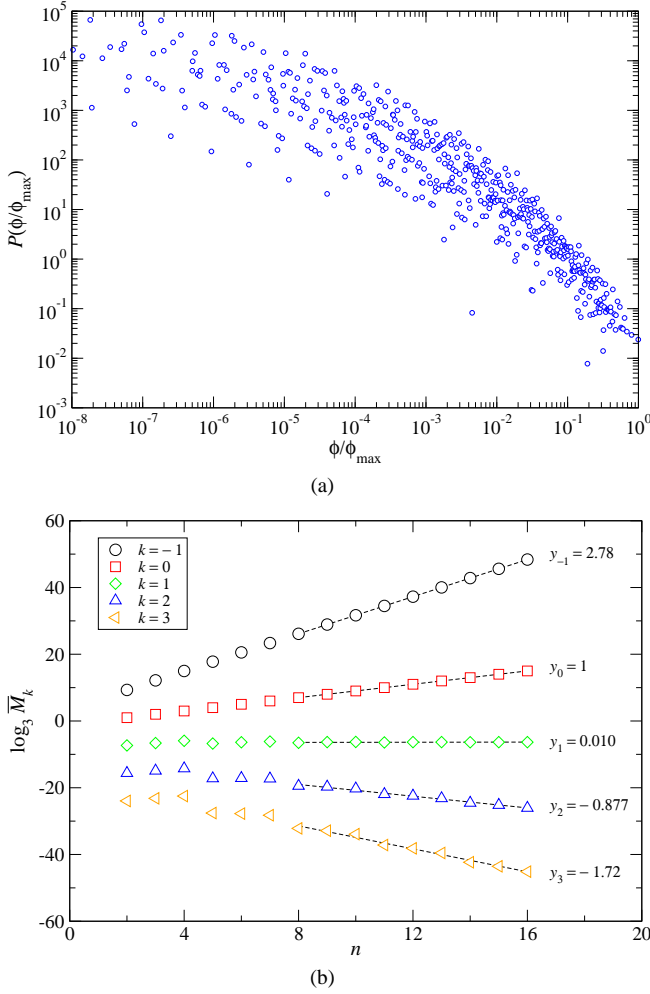


Figure 4: (a) Flux distributions in a given layer, re-scaled by the corresponding maximum flux, for  $q = 2$  and  $n = 22$ . (b) Moments of the flux as a function of  $n$ , for  $q = 3$  and several values of  $k$ , with the corresponding exponents  $y_k$ . Notice that there is no linear relation between the exponents.

we have

$$\bar{M}_k(L) \sim L^{y_k}, \quad (28)$$

with  $y_k = u_k/\ln 3$ . For  $q = 1$ , all sites in a given layer  $n$  have the same flux  $3^{-n}$ , so that the exponents  $y_k$  are given by  $y_k = 1 - k$ . For  $q \geq 2$ , on the other hand, we see from our numerical calculations that there is no simple linear relation between the exponents  $y_k$ , suggesting that no single number characterizes the current distribution. This is a signature of multifractal behavior. A plot of  $\bar{M}_k(n)$  for  $q = 3$  and several values of  $k$  is shown in Fig. 4(b).

To further investigate the multifractal properties of the flux distribution, we evaluate the multifractal spectrum  $f(\bar{\alpha})$ , defined by a Legendre transform of the exponents  $y_k$ ,

$$f(\bar{\alpha}) = y_k + k\bar{\alpha}, \quad \bar{\alpha} = -\frac{dy_k}{dk}. \quad (29)$$

Plots of  $f(\bar{\alpha})$  for several values of  $q$  are shown in Fig. 5. Note

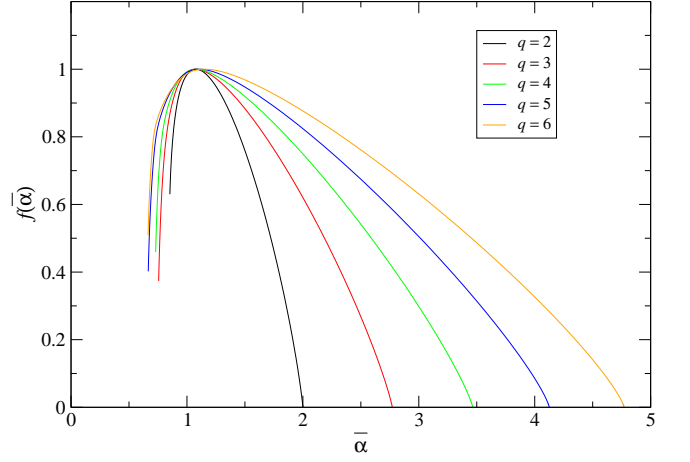


Figure 5: Plots of  $f(\bar{\alpha})$  for different values of  $q$ .

that, according to Eq. (29), the maximum of  $f(\bar{\alpha})$  occurs for the value of  $\bar{\alpha}$  associated with  $k = 0$ , for which  $f(\bar{\alpha}_{k=0}) = y_0$ . Indeed, for  $q = 1$  (not shown in Fig. 5), the curve consists of a single point,  $(\bar{\alpha}_{k=0}, y_0) = (1, 1)$ , corresponding to a monofractal behavior. Within numerical errors, that point is the maximum of all curves, in agreement with the fact that  $y_0 = 1$  for all values of  $q$ .

For  $q \geq 2$ , the left (right) end of the curves reflects the scaling behavior of the set of points associated with the largest (smallest) fluxes. Although not visible in the plots, the density of points is much larger near the ends of the curves, with intermediate points coming mostly from values of  $k$  between  $-1$  and  $0$ . The width of the curves increases with  $q$ , presumably diverging as  $q \rightarrow \infty$ . This is related to the fact that larger values of  $q$  lead to a larger range of values of the flux in each layer of the lattice.

## V. CONCLUSIONS

In this work we investigate directed sandpile models on the Apollonian network. Exact results were obtained for the avalanche distributions when  $q = 1$  and  $2$ . These correspond to the situations where an unstable node topples only to neighbors introduced in the first and the second subsequent generations, respectively. The avalanche distributions follow power-law behavior, with typical mean field exponents. The iteration of the exact expression for the two and three point correlation function provides evidences for the same asymptotic behavior, regardless of the finite value of  $q$ . On the other hand, our results also show the emergence of large oscillatory deviations due to finite size effects. This general behavior can be explained by noting that any finite value of  $q$  asymptotically constraints the sandpile model on the Apollonian network to the structure of a tree, where it behaves like a mean field model.

The investigation of the local properties of the fluxes through each node shows that the network geometry induces a large degree of inhomogeneity in the sandpile model. This

effect has not been observed for the same model in Euclidian lattices. Nevertheless, this dependence can be accurately accounted for by a multifractal analysis. Only for  $q = 1$ , when the model is equivalent to that defined on a Cayley tree, all nodes become indistinguishable, and the scaling analysis reduces to a single point.

Finally, the comparison with results found for another sandpile model on scale-free networks [?] shows similarities, in the mean field behavior when all nodes share the same critical height or the critical height depends locally on the node degree.

### Appendix A: ANALYTICAL TREATMENT FOR $q = 2$

For  $q \geq 2$ , the sites in each layer of the Apollonian network can be grouped in types, according to how they are connected to their backwards neighbors. This feature can be exploited in order to obtain analytical results for the behavior of the directed sandpile model. Here we deal with the case  $q = 2$ , which allows us to check our numerical results in a reasonably simple way. It is clear that the treatment can be extended to higher values of  $q$ , with basically the same results, but a considerably larger amount of work.

Layer  $n = 1$  of the network contains only one site, while the three sites in layer  $n = 2$  are all equivalent. However, already for  $n = 3$  two types of sites are present: sites of type 1 receive grains from sites in the two previous layers, while sites of type 2 receive grains only from the latter layer; see Fig. 2. For  $n = 4$ , two additional types of sites would appear, since it is possible that a site receives grains from sites of types 1 or 2, in one or two of the previous layers. It is easy to convince oneself that the number of site types doubles for each additional layer (starting at  $n = 2$ ), and that the types can be labeled so that each site of type  $s$  has as nearest neighbors in the next layer two sites of type  $2s - 1$  and one site of type  $2s$ .

Denoting by  $g_{n,s}$  the value of  $G_0(\mathbf{x}; \mathbf{x}_0)$  for a site  $\mathbf{x}$  of type  $s$  in layer  $n$ , and by  $v_{n,s}$  the number of such sites, the flux through layer  $n$  can be written as

$$\phi(n) = \sum_{s=1}^{2^{n-2}} v_{n,s} g_{n,s}. \quad (\text{A1})$$

In order to estimate  $\phi(n)$ , we must investigate the asymptotic behavior of both  $v_{n,s}$  and  $g_{n,s}$ .

Our choice of labels allows us to write, for  $s = 2j - 1$  ( $j = 1, 2, 3, \dots$ ),

$$g_{n,2j-1} = \frac{1}{9} \left( g_{n-1,j} + g_{n-2, \lfloor \frac{j+1}{2} \rfloor} \right), \quad v_{n,2j-1} = 2v_{n-1,j}, \quad (\text{A2})$$

in which  $\lfloor w \rfloor$  denotes the integer part of the number  $w$ , and, for  $s = 2j$ ,

$$g_{n,2j} = \frac{1}{9} g_{n-1,j}, \quad v_{n,2j} = v_{n-1,j}. \quad (\text{A3})$$

Equations (A2) and (A3), being recursive expressions, can be solved numerically to yield all  $g_{n,s}$  and  $v_{n,s}$  in terms of  $g_{1,1}$

and  $v_{1,1}$ . However, analytical results can be derived from the observation that  $g_{n,1}$  behaves as

$$g_{n,1} \sim \zeta^n, \quad (\text{A4})$$

with  $\zeta = (1 + \sqrt{37})/18 \simeq 0.393$  being determined from the solution of the equation

$$\zeta^2 = \frac{1}{9}(\zeta + 1). \quad (\text{A5})$$

Consequently,  $g_{n,s}$  satisfies

$$g_{n,s} \simeq A_s \zeta^n, \quad (\text{A6})$$

with constant prefactors  $A_s$ . Moreover, the multiplicities  $v_{n,s}$  are such that  $v_{n,1} = 3 \cdot 2^{n-2}$  ( $n \geq 2$ ) and the ratios  $f_s \equiv v_{n,s}/v_{n,1}$  satisfy

$$\begin{cases} f_{2j-1} = \frac{v_{n,2j-1}}{v_{n,1}} = \frac{2v_{n,j}}{2v_{n,1}} = f_j, \\ f_{2j} = \frac{v_{n,2j}}{v_{n,1}} = \frac{v_{n,j}}{2v_{n,1}} = \frac{1}{2}f_j. \end{cases} \quad (\text{A7})$$

We can rewrite Eq. (A1) as

$$\phi(n) = v_{n,1} \sum_{s=1}^{2^{n-2}} f_s g_{n,s} = v_{n,1} \sum_{m=0}^{n-2} \Gamma_{n,m}, \quad (\text{A8})$$

with

$$\Gamma_{n,0} = g_{n,1} \quad \text{and} \quad \Gamma_{n,m} = \sum_{s=1+2^{m-1}}^{2^m} f_s g_{n,s} \quad (m \geq 1). \quad (\text{A9})$$

Making use of the definition of  $\Gamma_{n,m}$  and of Eqs. (A2), (A3) and (A7), we can obtain the recursion equation

$$\Gamma_{n,m} = \frac{1}{6}(\Gamma_{n-2,m-2} + \Gamma_{n-1,m-1}). \quad (\text{A10})$$

Keeping in mind Eq. (A6), we expect that  $\Gamma_{n,m}$  takes the asymptotic form

$$\Gamma_{n,m} \simeq \gamma_m \zeta^n. \quad (\text{A11})$$

Substituting this last expression into Eq. (A10), we conclude that the constants  $\gamma_m$  satisfy the equation

$$\gamma_m \zeta^2 - \frac{1}{6} \gamma_{m-1} \zeta - \frac{1}{6} \gamma_{m-2} = 0, \quad (\text{A12})$$

which can be solved by  $\gamma_m \simeq \gamma_0 \theta^m$ , with  $\theta = (2\zeta)^{-1}$ . We then have

$$\Gamma_{n,m} \sim \theta^m \zeta^n = \frac{1}{2^m} \zeta^{n-m}, \quad (\text{A13})$$

and the flux  $\phi(n)$  scales with the layer index as

$$\phi(n) \sim 2^n \cdot \zeta^n \sum_{m=0}^{n-2} \theta^m = (2\zeta)^n \frac{\theta^{n-1} - 1}{\theta - 1}. \quad (\text{A14})$$

Since  $\theta > 1$ , this is equivalent to

$$\phi(n) \sim (2\zeta\theta)^n = 1, \quad (\text{A15})$$

so that the flux becomes asymptotically constant for  $n \gg 1$ .

The function  $K(n)$ , defined by

$$K(n) = \sum_{\mathbf{x} \in n} G_0(\mathbf{x}; \mathbf{x}_0) G_0(\mathbf{x}; \mathbf{x}_0) = \sum_{s=1}^{2^{n-2}} v_{n,s} g_{n,s}^2, \quad (\text{A16})$$

scales as  $K(n) \sim \zeta^n$ , and thus vanishes exponentially for large  $n$ . In the same limit, the function  $F(n)$ , related to  $K(n)$  and  $\phi(n)$  through the equation

$$\sum_{t=1}^n F(t) K(n-t+1) = \phi(n), \quad (\text{A17})$$

tends to a constant value. As a consequence, the mean square flux must scale as

$$\Phi(n) = \sum_{t=1}^n F(n) [\phi(n-t+1)]^2 \sim n, \quad (\text{A18})$$

yielding the mean-field exponent  $\alpha = 1$ .

## ACKNOWLEDGMENTS

This work was partially financed by the Brazilian agencies CNPq, FUNCAP, and FAPESB. HJH acknowledges the support of the Max Planck prize.